LA-UR- 99- 333

Approved for public release; distribution is unlimited.

CONF-990110--

Title: SIMULATIONS OF LASER THROMBOLYSIS

Author(s): Edward J. Chapyak and Robert P. Godwin,
Group XNH, Applied Theoretical and
Computational Physics Division,
Los Alamos National Laboratory,
Los Alamos, New Mexico 87545

Submitted to: Proceedings of Lasers in Surgery IX,
Part of SPIE's International Symposium, BiOS'99,
23-29 January 1999, San Jose, CA
(SPIE #3590D-52)

Los Alamos
NATIONAL LABORATORY

DISCLAIMER

Word file -- BiOS'99 Sim. 01/15
SPIE #3590D-52 Draft submitted for FSS document approval

Simulations of Laser Thrombolysis

Edward J. Chapyak and Robert P. Godwin

Applied Theoretical and Computational Physics Division,
Los Alamos National Laboratory,
MS F664, Los Alamos, NM 87545

ABSTRACT

We have shown that bubble expansion and collapse near the interface between two materials with modest property differences produces jet-like interpenetration of the two materials. The bubble dynamics at a water-viscous fluid interface is compared with that at the interface of water with a weak elastic-plastic material. We find that, despite rather similar behavior during bubble growth and the initial portion of bubble collapse, the terminal jetting behavior is quite different, even in direction. The elastic-plastic properties chosen realistically represent real and surrogate thrombus. Simulations using the elastic-plastic model quantitatively agree with laboratory thrombolysis mass removal experiments. In our earlier simulations of laboratory experiments, walls have been remote so as to not effect the dynamics. Here we present two-dimensional simulations of thrombolysis with water over elastic-plastic surrogate thrombus in a geometry representative of the clinical situation. The calculations include thin cylindrical elastic walls with properties and dimensions appropriate for arteries. The presence of these artery walls does not substantially change the interface jetting predicted in unconfined simulations.

Keywords: bubble dynamics, cavitation, confinement, jet formation, hydrodynamics, laser thrombolysis, material properties, numerical methods, tissue properties, wall effects

1. INTRODUCTION

Laser thrombolysis has been under development for about ten years as a treatment for acute myocardial infarction (AMI) and ischemic stroke.[1] Despite a decade of study, the photomechanical processes dominating laser-driven clot removal were not clearly identified until recently. Laboratory thrombolysis experiments carried out at the Oregon Medical Laser Center (OMLC) over the last few years show that, above the energy threshold for bubble formation, the mass removal process is insensitive to the experimental parameters. The laser mass removal efficiency is nearly constant for a given experimental geometry and surrogate clot absorption coefficient and is ~2 μg/mJ.[2] This result holds for various laser wavelengths and for pulse lengths from 1 μs to 10 ms.[3] Framing photographs indicate the mass removal occurs during a volcanolike ejection of clot hundreds of microseconds after delivery of the laser energy. Analysis and numerical simulations indicate these experimental features are convincing evidence that jetlike interface dynamics driven by bubble dynamics dominates laser thrombolysis (and certain other laser procedures involving soft tissues). The collapse dynamics of the vapor bubble produced by the laser deposition drives a jet from the clot into the overfluid removing clot mass in the process.[2,4] Kodama et al.[5] have studied a thrombolysis procedure in which an overfluid jet is driven into clot eroding the clot in the manner of armor piercing munitions.[6] The jet is produced by dictating the collapse dynamics of a bubble located in front of the clot with a chemical explosion having an energy of a few joules.

In Sec. 2, we review our previous numerical investigations and compare the results with OMLC experimental photographs. We illustrate the importance of appropriate tissue models for

simulating bubble-driven tissue dynamics by comparing the markedly different collapse jets obtained using viscous and elastic-plastic properties to model the surrogate clot.

Previous work validated our numerical tools for bubble-driven dynamics by comparison of simulations with analytical test problems based upon the Rayleigh-Plesset equation and with OMLC experiments in unconfined geometry. We have also validated our approach of initializing the dynamics with a seed bubble, designed to produce a maximum bubble size typical of those produced in the OMLC experiments. We have now more realistically simulated clinical laser thrombolysis. In Sec. 3.1, we present simulations of laser thrombolysis which include an arterial wall in the numerical model. Simulations of bubble dynamics inside a rigid tube are presented in Sec. 3.2. In Sec. 4, we summarize the status of computationally modeling laser-thrombolysis and other laser-medical applications in which bubble dynamics is important.

2. REVIEW: THE IMPORTANCE OF TISSUE RESPONSE MODELS

Figure 1 displays thrombolysis photographs taken at the OMLC near the time of the maximum laser-produced bubble volume and at approximately twice that time (that is, when an isolated bubble would collapse to its minimum volume). Also shown are Los Alamos MESA2D code snapshots at the comparable times from a simulation described in Ref. 4. Elastic-perfectly plastic material response was assumed in modeling the gelatin surrogate clot. The elastic-plastic tissue response parameters chosen were based upon experiments. The agreement between the experiments and simulations is striking. Upon careful examination of the experimental photograph taken at collapse, one sees even the "arms" of water which are evident outside the upward moving gelatin jet in the simulation. One might incorrectly deduce from the experimental photograph that the maximum hemi-spherical bubble volume in the gelatin is approximately equal to the hemi-spherical volume in the water and that this disagrees with the simulation. In the simulation, the hemi-sphere in the "elastic-plastic clot" is significantly smaller than the hemi-sphere in water. The experimental hemi-spherical bubble in gelatin is smaller than the hemi-sphere in water. The dyed layer of the experimental sample has been pushed down into the clear gelatin by bubble expansion, so that what appears to be the bubble-gelatin interface is in fact the interface of dyed and clear gelatin. The true bubble-gelatin interface cannot be seen in the photo.

In Fig. 2, we illustrate the dramatic effect of material properties on late-time bubble-driven interface dynamics. The upper and lower rows of numerical snapshots are from simulations using identical high-pressure seed bubbles. In the simulation of the upper row (described in Ref. 7), the surrogate clot was simulated as water with an artificially high viscosity. In the lower row, surrogate clot was modeled as an elastic-perfectly plastic material with parameters characteristic of real gelatin or clot (shear modulus μ=0.4 bar and plastic flow stress Y=0.1 bar).[4] Comparing the two rows of Fig. 2 demonstrates that care must be used in validating numerical tissue response models against experimental data. At the time of maximum bubble volume (and all earlier times), the two models for surrogate clot yield bubble dynamics histories which agree very well with each other and with experimental records. The bubble dynamics of the two simulations using very diffferent strength models even agree fairly well at 170 μs, that is, through more than 90% of the bubble's growth-collapse period. At 180 μs, near the collapse time of an isolated bubble in water, the situation has changed. The simulation using a viscous model produces a pair of water jets moving away from the gel-water interface in opposite directions. This simulation bears no resemblance to experimental results. On the other hand, the simulation using an elastic-perfectly plastic model produces a jet of gelatin into the water in excellent agreement with OMLC experiments. Details of the surrogate tissue response model employed in simulations dominate the all important final collapse dynamics.

We predicted from parametric simulation studies that bubble collapse at the interface of fluids with different densities, but otherwise similar properties, would produce a jet from a lower density into a higher density fluid.[4] Thus, if a low-density low-viscosity fluid overlays a weak elastic-plastic material, such as gelatin or clot, slight changes in material properties may cause the direction of collapse jets to change. This situation occurred in Los Alamos experiments comparing bubble dynamics at the interface of low-density low-viscosity oil with gelatin surrogate clot, a surrogate clot developed by Trajkowska, and real clot.[8] In otherwise similar experiments, oil jetted into gelatin upon bubble collapse, while Trajkowska's surrogate clot and real clot jetted into the oil. Apparently the gelatin was enough weaker than the other surrogate and real clot to allow the low-density oil to dictate jetting in the gel experiment, while in the other two cases clot strength dictated the jetting.

Tissue dynamics similar to that of thrombolysis experiments and simulations has been observed in other laser-coupling experiments involving soft tissue.[9] Simulations using elastic-plastic tissue response explain bipolar pressure waves observed after laser breakdown in corneal tissue, whereas simpler response models do not.[10]

3. SIMULATIONS IN CYLINDRICAL TUBES

3.1. Elastic surrogate artery walls

The studies reviewed above provided an understanding of the fundamental physical mechanisms dominating laser thrombolysis and demonstrated that our numerical simulation tools can model experiments in unconfined geometries. We now describe numerical calculations which more realistically simulate clinical laser thrombolysis. The same high pressure, spherical seed bubble which we have used in our earlier studies initiated the bubble dynamics.[11] The dynamic response of clot surrogate was modeled with the elastic-plastic parameters used in the unconfined simulations discussed above. Now, however, we introduced thin-walled elastic cylinders into our simulations as surrogate artery walls. The tubes have an inner diameter of 2 mm and a 0.2 mm wall thickness. We have used elastic response with a shear modulus of 2.0 bar = 0.2 MPa = 2×10^5 N/m^2 as an elementary approximation to the complex non-linear response of artery walls.[12,13] Figure 3 displays numerical snapshots near the maximum bubble volume and at a time slightly after the collapse time of an isolated bubble in water. We have compared these snapshots with snapshots taken at the same time for an unconfined, but otherwise identical, simulation. At 90 μs, that is, at near maximum bubble volume, the confined and unconfined simulation bubbles are very similar. The bubble in the elastic tube simulation is slightly smaller because energy was expended in pushing out the elastic tube wall. At 200 μs, similar well-defined jets of gelatin into the water and toward the optical fiber exist in both the confined and unconfined simulations. The jet in the confined case appears to be slightly less vigorous, but the difference is minor. The predicted mass removal dynamics is qualitatively unchanged by the addition of the elastic vessel to the numerical model.

Vogel et al.[14] experimentally investigated a situation similar to that which we have modeled. They studied the cavitation dynamics produced by 70 mJ 3 μs 630 nm laser pulses in water within elastic silicone tubes immersed in water. The laser pulses created bubbles comparable in radius to the elastic tubes which had a 5 mm outer diameter and a 0.4 mm wall thickness. The Young's modulus of the tubes was 2×10^6 N/m^2, close to that of vessels. The tube and bubble dynamics observed were similar to those in our simulations, but with two easily understood exceptions. The first exception being the interface jetting in our simulations at the interface of gel and water upon bubble collapse. The second is the presence in the experiments of cavitation external to the elastic tube during bubble collapse. We are confident that, if we modeled uniform water within the tube and placed an appropriate numerical floor (~1 to 10 bar) on the tensile stress water can withstand, our computational tools could easily be matched to Vogel's single-

pulse experiments. In the Vogel experiments and in our simulations with elastic tube walls, the bubble growth-collapse oscillation time was qualitatively similar to that of an isolated bubble. Energy stored in the elastic wall during bubble growth is returned during collapse leaving the oscillation time nearly unchanged.

3.2. Rigid tube walls

While artery walls and most other tissues of interest in laser-medical applications are relatively soft, containers with rigid walls are often used in laboratory studies of laser-tissue coupling. For example, OMLC bubble dynamics experiments supporting laser thrombolysis and drug delivery studies were carried out in long 1x1 cm^2 cross section cuvettes.[15] The radial growth-collapse oscillation period of bubbles produced by identical laser pulses was compared for bubbles produced in these cuvettes and in a large fluid volume. The bubbles in the large experimental volume exhibited the familiar oscillation with a period approximately twice the Rayleigh time, that is, $T(\mu s) \approx 183 R_o$, where R_o is the bubble's maximum radius in millimeters.[16] The maxium dimensions of the bubbles studied were $\leq 1/3$ those of the confining vessel. As shown in Fig. 4, confinement in a vessel with rigid walls significantly changes the bubble dynamics. The maximum bubble diameter, measured with respect to the symmetry axis of the experiment, was ~3/4 that of the unconfined bubble and the oscillation period was prolonged by at least 50%. A prolongation of the period is expected, since a nearby planar wall prolongs the oscillation period of a bubble by as much as 20%.[16,17] It is, therefore, not surprising that 360° radial confinement has an even greater effect on the oscillation period.

Using the MESA code, we have numerically investigated the dynamics of a high-pressure spherical seed bubble in water as a function of the radius a rigid cylindrical confining vessel. As in many of our earlier studies, the numerical seed bubble contained an ideal gas with γ=1.4 at a pressure of 505 bar and had a radius of 0.1 mm. In Fig. 5, the radius of a spherical bubble with a volume equal to the volume of the simulation bubble is plotted as a function of time for confinement radii of 2, 5, and 25 mm. The bubble dynamics of the 25 mm case is virtually identical to that in an infinite water volume. The 2 and 5 mm radius cases yielded oscillation period prolongation factors of about 1.9 and 1.2, respectively, compared to the period of an unconfined bubble. A quantitative comparison cannot be made between the OMLC experiment in a tube of square cross section and our cylindrical simulation. However, as one would expect, the bubble dynamics of the 2 mm radius simulation is qualitatively similar to that of the OMLC experiment in the square cuvette. The simulations of bubble dynamics exhibited several features worthy of further numerical study. The oscillations in the spherized radius temporal history curves for the 2 and 5 mm tubes are interesting as is the fact that bubble collapse in the confined cylindrical geometries was numerically unstable.

4. SUMMARY: THE STATUS OF NUMERICAL MODELING

Our understanding and numerical modeling of laser thrombolysis have matured. We can confidently state that we understand and can reliably model the bubble-driven hydrodynamics which dominates the clot removal process. If sufficiently realistic laser energy deposition models and dynamic response models for clot, artery walls, and other important clinical features were coupled to our numerical hydrodynamics and equations of state, we would be able to provide engineering studies of clinical laser thrombolysis. Engineering modeling would, however, require large computational resources. Expensive computing is needed to resolve spatial details of catheter design, etc. and for three-dimensional modeling. Our simulations to date have used two-dimensional cylindrical symmetry and have been sufficiently realistic and accurate to identify the fundamental processes of thrombolysis. This situation has pertained because the catheters used to deliver laser energy to the thrombi causing AMI and ischemic stroke and arteries have near cylindrical symmetry. Nevertheless, we expect three-dimensional

effects to occur for bubbles off the axis of symmetry of even a cylindrical vessel. Thrombi are inhomogeneous and irregular in shape, and thus, have intrinsic three-dimensional features. Computational hardware and software resources for modeling such three-dimensional effects are rapidly becoming more common and less expensive, especially in major interdisciplinary centers, such as Los Alamos.

ACKNOWLEDGMENTS

This work was supported in part by a Cooperative Research and Development Agreement (CRADA) between Los Alamos National Laboratory (Department of Energy), Oregon Medical Laser Center, and Palomar Medical Technologies. We dedicate this work to HanQun Shangguan, a member of the CRADA team until his recent untimely death.

REFERENCES

1. K. W. Gregory, Vol. 2 Chap. 53, "Laser Thrombolysis," *Textbook of Interventional Cardiology 2nd Ed.*, edited by E. J. Topol, Saunders, Philadelphia, 1994.
2. R. P. Godwin, E. J. Chapyak, S. A. Prahl, and H. Shangguan, "Laser Mass Ablation Efficiency Measurements Indicate Bubble-Driven Dynamics Dominates Laser Thrombolysis," *Lasers in Surgery: Advanced Characterization, Therapeutics, and Systems VIII, Proc. SPIE* **3245**, pp. 4-11, 1998.
3. J. A. Viator and S. A. Prahl, "Laser thrombolysis using a millisecond frequency-doubled Nd-YAG laser," *Laser Tissue Interaction IX, Proc.SPIE* **3254**, pp. 287-291, 1998.
4. E. J. Chapyak and R. P. Godwin, "Physical Mechanisms of Importance to Laser Thrombolysis," *Lasers in Surgery: Advanced Characterization, Therapeutics, and Systems VIII, Proc. SPIE* **3245**, pp. 12-18, 1998.
5. T. Kodama, K. Takayama, and H. Uenohara, "A new technology for revascularization of cerebral embolism using liquid jet impact," *Phys. Med. Biol.* **42**, pp. 2355-2367, 1997.
6. R. P. Godwin and E. J. Chapyak, "Apparent Target Strength in Long-Rod Penetration," *Int. J. Impact Engng.* **21**(1-2), pp. 77-88, 1998.
7. E. J. Chapyak, R. P. Godwin, S. A. Prahl, and H. Shangguan, "A Comparison of Numerical Simulations and Laboratory Studies of Laser Thrombolysis," *Lasers in Surgery: Advanced Characterization, Therapeutics, and Systems VII, Proc. SPIE* **2970**, pp. 28-34, 1997.
8. R. E. Hermes and K. Trajkovska, "Synthetic thrombus model for *in vitro* studies of laser thrombolysis," *Laser Tissue Interaction IX, Proc.SPIE* **3254**, pp. 211-217, 1998. See Fig. 3.
9. M. CM. Grimbergen, R. M. Verdaasdonk, and C. F.P. van Swol, "Correlation of thermal and mechanical effects of the holmium laser for various clinical applications," *Laser Tissue Interaction IX, Proc.SPIE* **3254**, pp. 69-79, 1998. See Fig. 8.
10. Vogel, R. J. Scammon, and R. P. Godwin, "Tensile stress generation by optical breakdown in tissue: Experimental investigations and numerical simulations," *Laser Tissue Interaction X, SPIE* **3601**, 1999 (to be published).
11. E. J. Chapyak and R. P. Godwin, "Numerical Studies of Bubbles in Laser Thrombolysis," *Lasers in Surgery: Advanced Characterization, Therapeutics, and Systems VI, Proc. SPIE* **2671**, pp. 84-87, 1996.
12. Y. C. Fung, Chap. 8, "Mechanical Properties and Active Remodeling of Blood Vessels," *Biomechanics: Mechanical Properties of Living Tissues, 2nd Ed.*, Springer, New York, 1993.
13. R. E. Shadwick, "Elasticity in Arteries," *Am. Sci.* **86**(6), pp. 535-541, Nov.-Dec. 1998.
14. A.Vogel, R. Engelhardt, U. Behnle, and U. Parlitz, "Minimization of cavitation effects in pulsed laser ablation illustrated on laser angioplasty," *Appl. Phys.* **B62**, pp. 173-182, 1996.
15. H. Shangguan and S. Prahl, Oregon Medical Laser Center (private communication).
16. R. H. Cole, Chap. 8, "Motion of the Gas Sphere," *Underwater Explosions*, Princeton U, Princeton, 1948.

17. R. P. Godwin, E. J. Chapyak, J. Noack, and A. Vogel, "Aspherical bubble dynamics and oscillation times," *Laser Tissue Interaction X, SPIE* **3601**, 1999 (to be published).

FIGURE CAPTIONS

The figures will be cleaned up for the oral presentation and for insertion in the final manuscript submitted for publication.

Fig. 1. Comparison of an OMLC laboratory laser thrombolysis experiment and a MESA2D numerical simulation. Red-dyed gelatin is the experimental surrogate clot and the overfluid is water. The simulation used an elastic-perfectly plastic dynamic response model for the clot with model parameters derived from experiment. The upper snapshots are near the time of maximum bubble volume, the lower snapshots near the collapse time of an isolated bubble in water. Note the vigorous bubble collapse jet carrying clot mass upward into water in both experiment and simulation.

Fig. 2. Comparison of snapshots from two simulations of the bubble dynamics driven by a seed bubble. In the simulation of the upper row, the clot was modeled as water with an artificially high viscosity. The snapshots of the lower row are from the same simulation as Fig. 1 using elastic-perfectly plastic clot response. Until beyond the time of maximum bubble volume (~90 μs) the two simulations are very similar to one another and to experimental photos. However, the bubble collapse-driven jetting of the viscous simulation bears no resemblance to experiment. On the other hand, the simulation using an elastic-perfectly plastic clot model produces a jet in excellent agreement with OMLC experiments.

Fig. 3. Numerical snapshots of a seed bubble-driven thrombolysis simulation identical to that of Fig. 1, except that an elastic surrogate artery has been added. The snapshots shown are near the maximum bubble volume and at a time slightly after the collapse time for an isolated bubble in water. The jetlike clot removal dynamics of Fig. 1 has been only slightly modified by the addition of artery walls.

Fig. 4. Measured bubble size as a function of time in OMLC experiments. The bubble history in a large fluid volume is compared with that of a bubble in a 1 cm square cuvette. The maximum bubble width measured in the cuvette was reduced to ~3/4 and the oscillation period prolonged by ~50% compared to the unconfined bubble. The fluid used was low-viscosity oil, but we believe qualitatively similar results would be found with water. (Unpublished data courtesy of S. Prahl, OLMC.)

Fig. 5. Radius of an equivalent spherical bubble as a function of time for dynamics initiated by a seed bubble in rigid tubes of radius 2, 5, and 25 mm. The 25 mm case is identical to that of an infinite water volume. In the 2 and 5 mm cases the oscillation period is prolonged by factors of about 1.9 and 1.2, respectively, compared to an unconfined bubble.

SNAPSHOTS AT MAXIMUM VOLUME AND DURING COLLAPSE [illegible]

OMLC Experiment
(Water / gelatin surrogate clot)

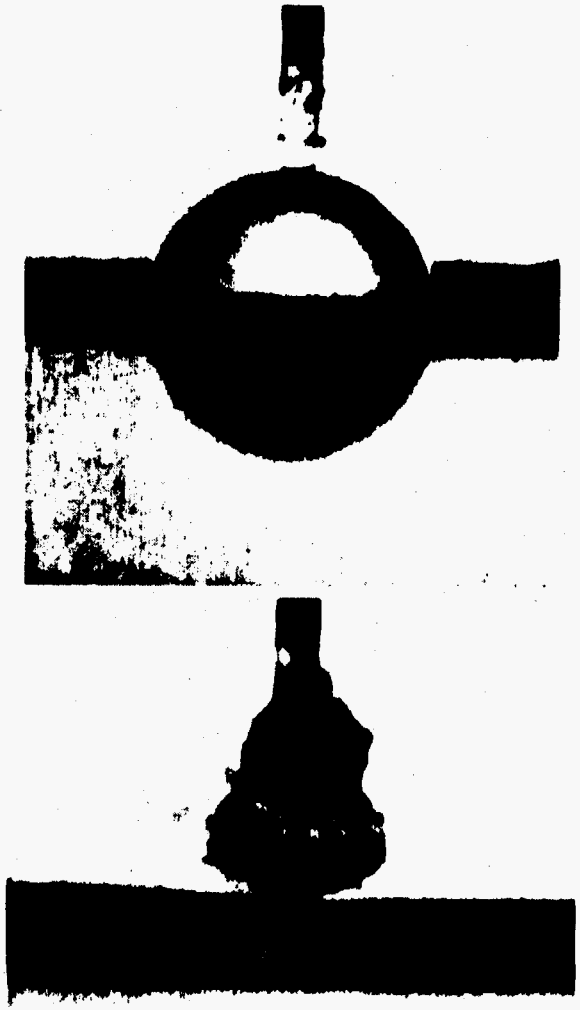

LANL Simulation
(Water / "Elastic - perfectly plastic clot")

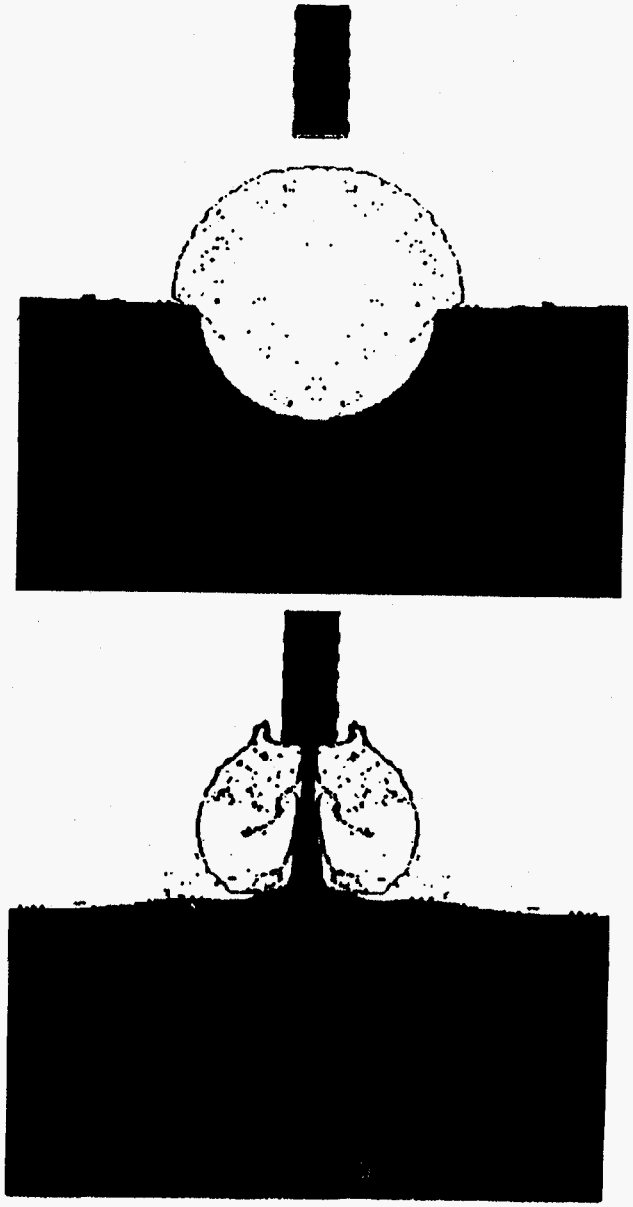

Fig. 1

Material properties strongly influence late-time collapse
Comparison of viscous and elastic-plastic case

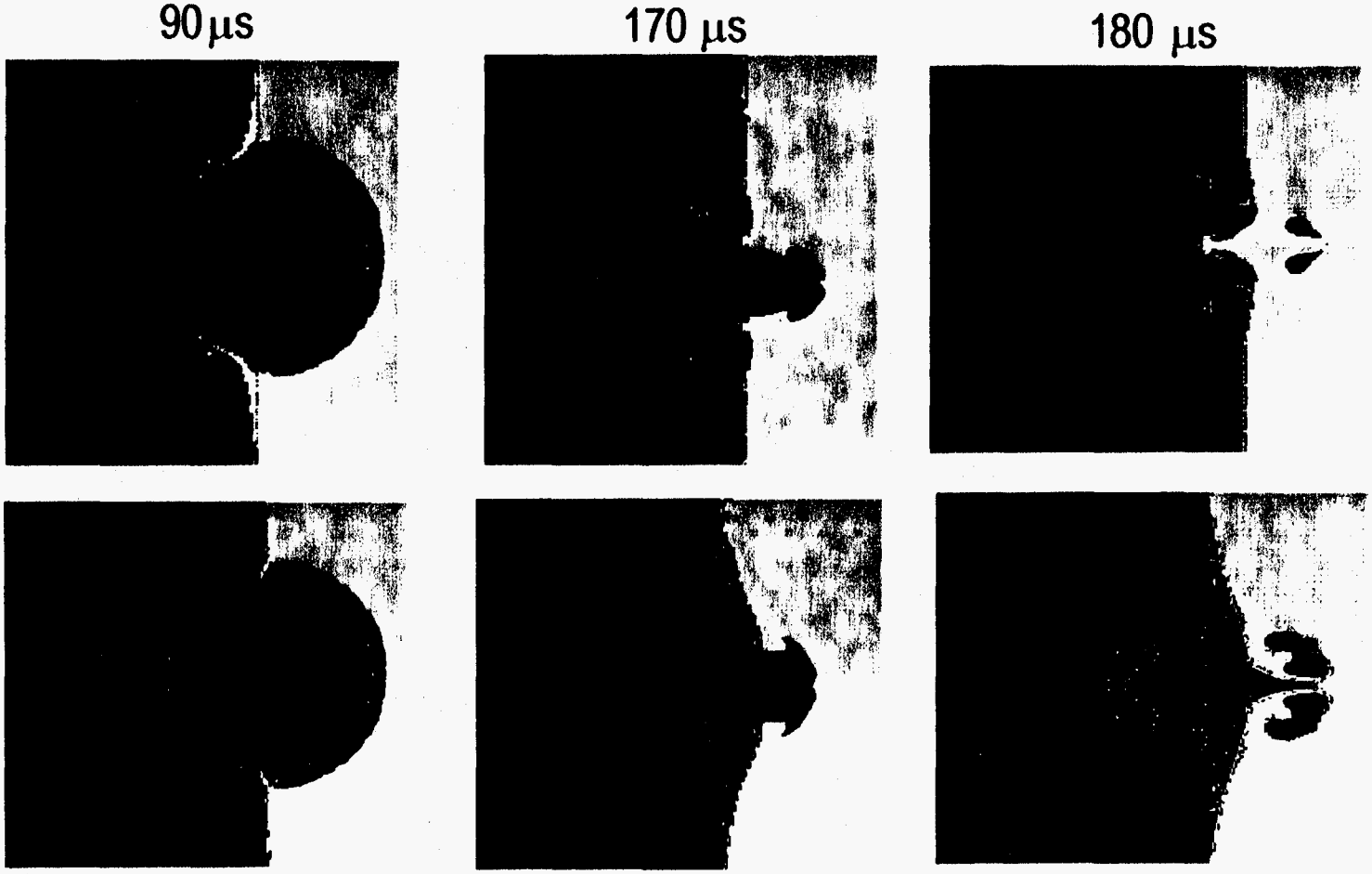

Fig. 7

/?

INTERFACES

time 90.0007

bub72 + 2mm artery (2.0 bar)

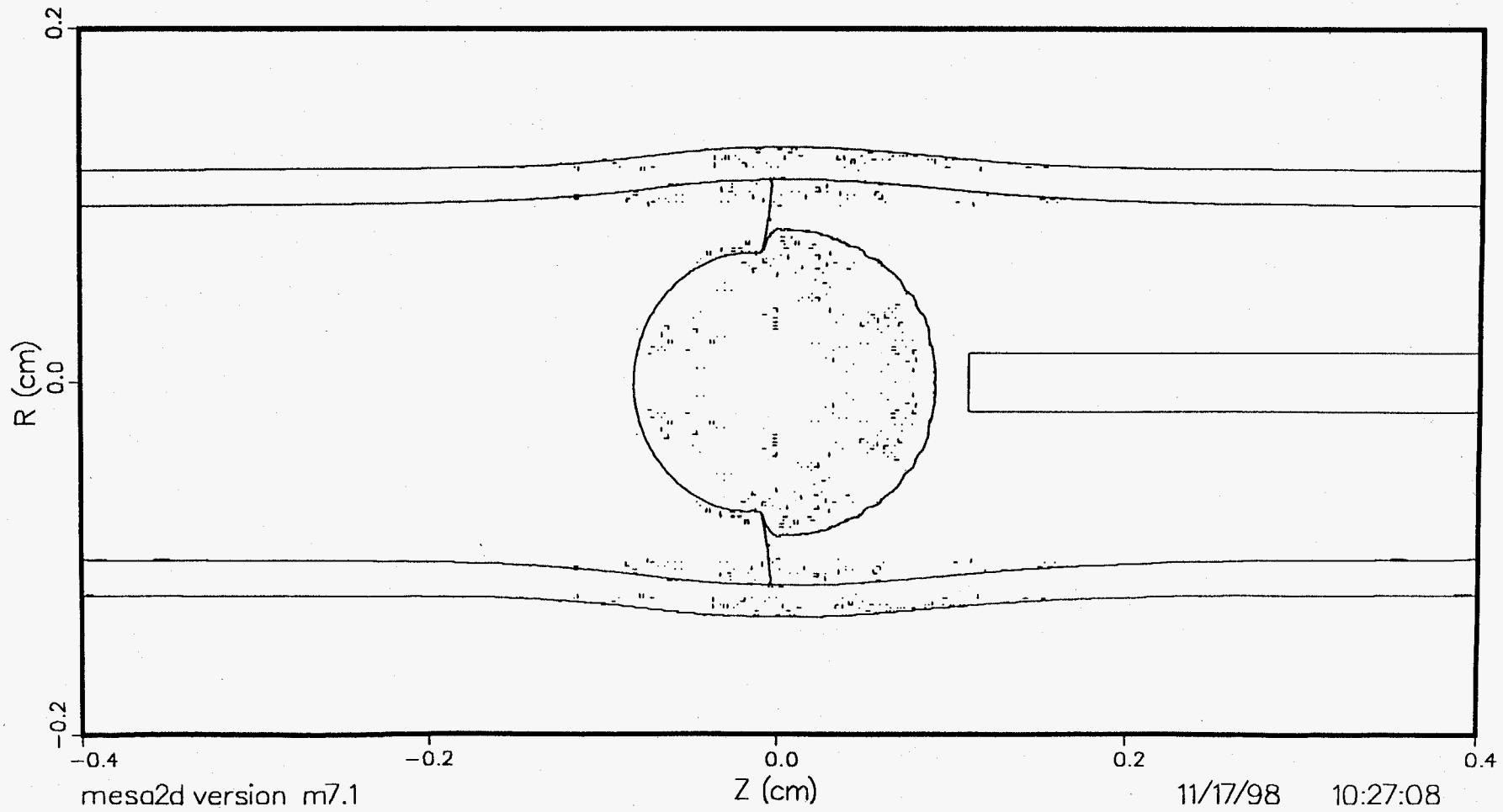

/?

INTERFACES

time 200.012

bub72 + 2mm artery (2.0 bar)

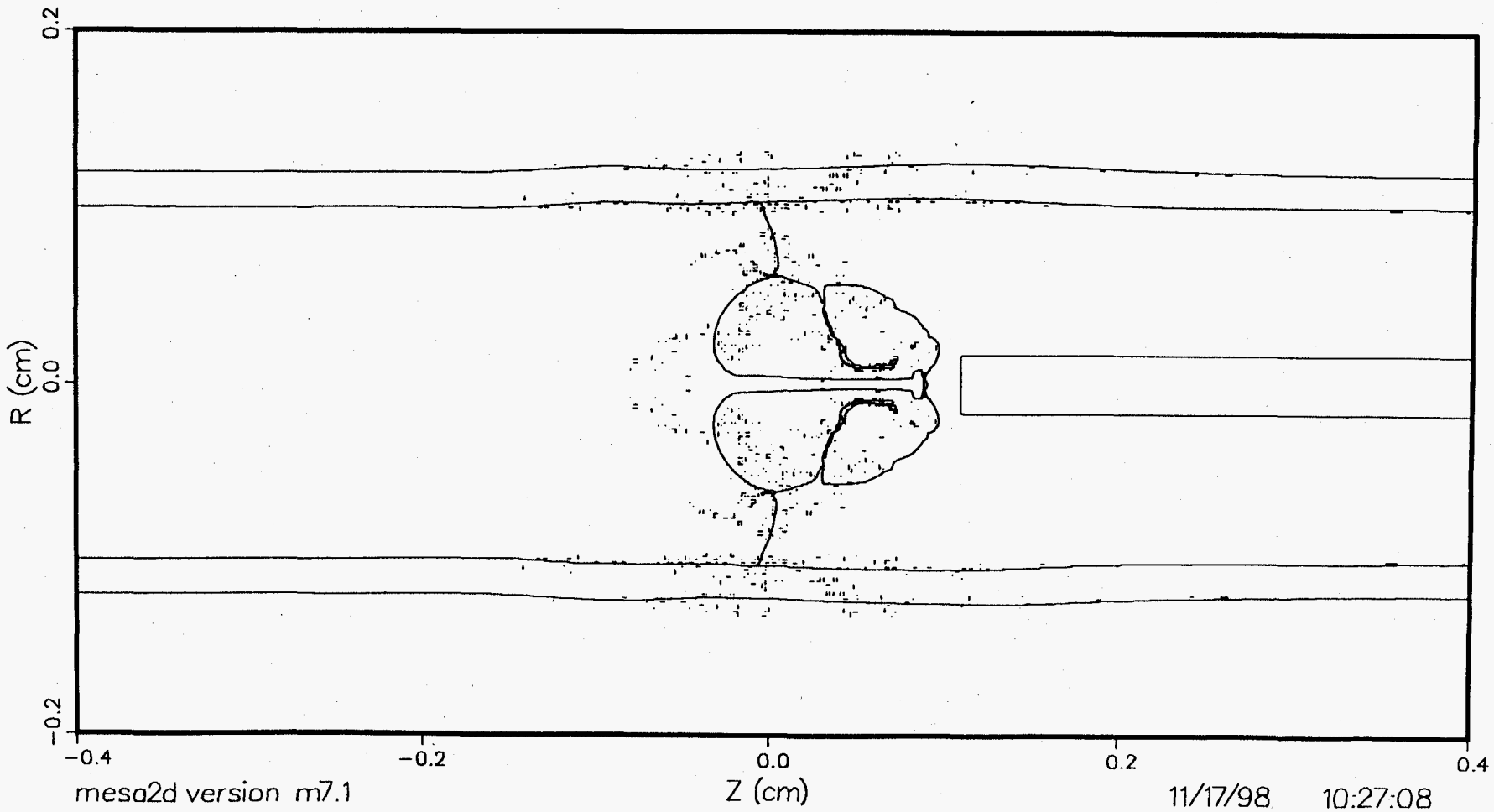

Fig. 36

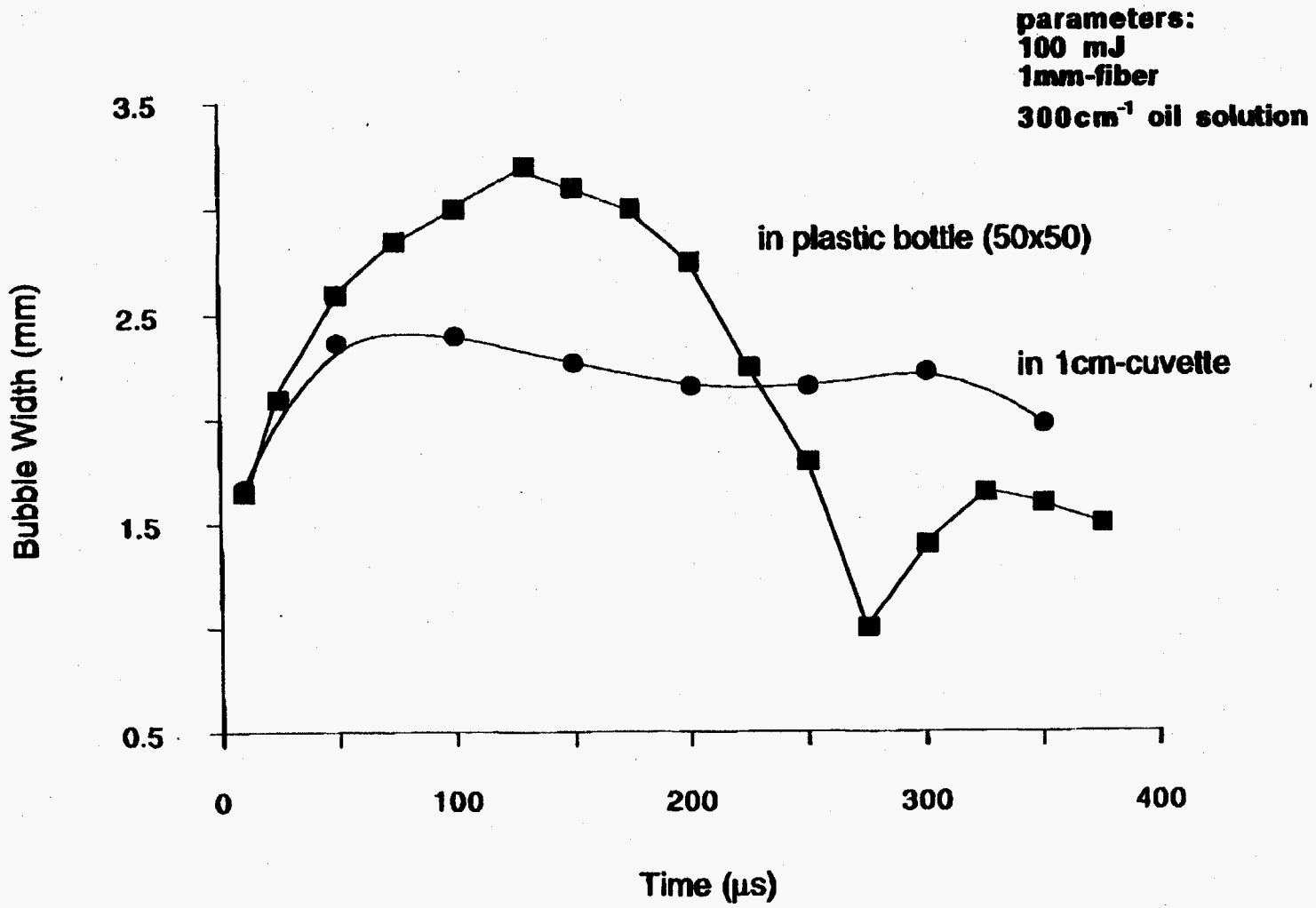
parameters:
100 mJ
1mm-fiber
300cm-1 oil solution
in plastic bottle (50x50)
in 1cm-cuvette
Bubble Width (mm)
3.5
2.5
1.5
0.5
0
100
200
300
400
Time (µs)

Fig. 4

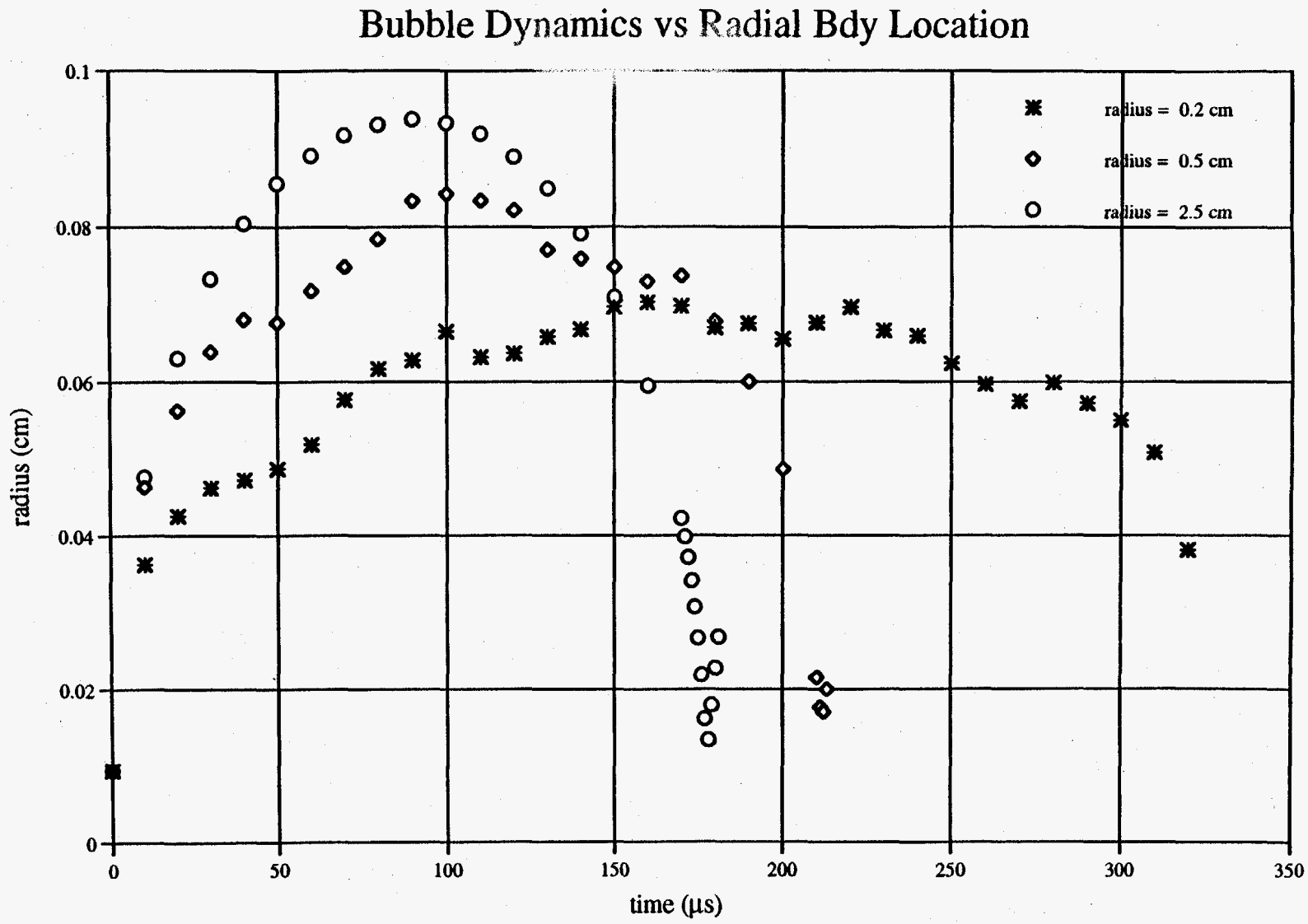
Bubble Dynamics vs Radial Bdy Location
radius (cm)
time (μs)
0.1
0.08
0.06
0.04
0.02
0
0
50
100
150
200
250
300
350
radius = 0.2 cm
radius = 0.5 cm
radius = 2.5 cm

Fig 5